



Published in final edited form as:

*J Vis.*; 9(2): 20.1–2016. doi:10.1167/9.2.20.

## Adaptive changes in visual cortex following prolonged contrast reduction

MiYoung Kwon<sup>1</sup>, Gordon E. Legge<sup>1</sup>, Fang Fang<sup>2</sup>, Allen M. Y. Cheong<sup>1</sup>, and Sheng He<sup>1</sup>

<sup>1</sup>Department of Psychology, University of Minnesota, Minneapolis, MN, USA

<sup>2</sup>Department of Psychology and Key Laboratory of Machine Perception (the Ministry of Education), Peking University, Beijing, China

### Abstract

How does prolonged reduction in retinal-image contrast affect visual-contrast coding? Recent evidence indicates that some forms of long-term visual deprivation result in compensatory perceptual and neural changes in the adult visual pathway. It has not been established whether changes due to contrast adaptation are best characterized as “contrast gain” or “response gain.” We present a theoretical rationale for predicting that adaptation to long-term contrast reduction should result in response gain. To test this hypothesis, normally sighted subjects adapted for four hours by viewing their environment through contrast-reducing goggles. During the adaptation period, the subjects went about their usual daily activities. Subjects' contrast-discrimination thresholds and fMRI BOLD responses in cortical areas V1 and V2 were obtained before and after adaptation. Following adaptation, we observed a significant decrease in contrast-discrimination thresholds, and significant increase in BOLD responses in V1 and V2. The observed interocular transfer of the adaptation effect suggests that the adaptation has a cortical origin. These results reveal a new kind of adaptability of the adult visual cortex, an adjustment in the gain of the contrast-response in the presence of a reduced range of stimulus contrasts, which is consistent with a response-gain mechanism. The adaptation appears to be compensatory, such that the precision of contrast coding is improved for low retinal-image contrasts.

### Keywords

contrast adaptation; contrast sensitivity; plasticity; visual cortex; contrast discrimination; fMRI; contrast gain; response gain; long-term visual deprivation

## INTRODUCTION

The ability to respond to visual contrast (i.e., differences in intensity between light and dark regions of an image) is crucial to many human visual activities including reading, object recognition and mobility. Contrast deprivation, in which the visual system is not able to receive or process a full range of contrast signals, is experienced by people with ocular-media disorders such as cataract or corneal scarring. The question arises whether prolonged reduction in retinal-image contrast affects visual-contrast coding. According to a simple *contrast attenuation model* (Rubin & Legge, 1989), only the range of effective contrast is reduced, but otherwise, visual perception and contrast coding are unaffected. There is, however, some evidence that afflicted individuals' subjective impressions of image contrast compensate for the attenuated visual input (Fine, Smallman, Doyle, & MacLeod, 2002; Hess & Bradley, 1980; Mei & Leat,

2007). In addition, some contrast-adaptation studies on a short time scale (hundreds of milliseconds to ten minutes) using both behavioral and neurophysiological methods support the view that the adaptation produces a functional benefit by enhancing contrast sensitivity around the adapting contrast (Gardner et al., 2005; Greenlee & Heitger, 1988; Heinrich & Bach, 2001; Pestilli, Viera, & Carrasco, 2007; Ross & Speed, 1991). It still remains to be determined how the adult visual system responds to prolonged contrast deprivation on the scale of hours, days or months.

### Compensation hypothesis

In this study, we tested a *compensation hypothesis*, that prolonged exposure to low contrasts results in compensatory changes in the adult human visual system. We examined the effects of prolonged contrast deprivation on contrast coding by having subjects with normal vision view the world through contrast-reducing goggles for 4 hours. Subjects' contrast-discrimination sensitivity and fMRI contrast response were measured in pre- and post-tests. Contrast discrimination thresholds are typically measured by determining the smallest contrast difference required to discriminate two patterns that are identical except for a difference in contrast. The plot of contrast increment threshold ( $\Delta C$ ) vs. baseline (i.e. pedestal) contrast ( $C$ ) is called the contrast discrimination function or threshold versus contrast (TvC) function. This function has a characteristic 'dipper shape' (Legge & Foley, 1980; Nachmias & Sansbury, 1974). It has been hypothesized that the shape of contrast discrimination functions is accounted for by the form of underlying neuronal contrast response functions (CRF) such that an increment in contrast ( $\Delta C$ ) can be detected only when the increment in the neuronal response increases by some criterion amount ( $\Delta R_c$ ) (Legge & Foley, 1980).

The first goal of the current study was to see whether prolonged exposure to low contrasts brings about any compensatory changes in visual contrast coding. If prolonged contrast reduction results in increased gain of the response in visual cortex—a form of neural compensation—then we would expect to see improved contrast discrimination, i.e. reduced values of  $\Delta C$ . If the adaptation occurs at the cortical level including binocular neurons, we should observe an interocular transfer effect of the adaptation to the unadapted fellow eye.

### Contrast gain or response gain?

Our second goal was to identify the mechanism of the prolonged adaptation. There are two likely mechanisms underlying any adaptive change: increased contrast gain and increased response gain. Often contrast adaptation has been studied on a short time scale of seconds or minutes. Its mechanism has often been described by a contrast-gain model in which the system adjusts the dynamic range of the CRF to be centered near the mean stimulus contrast. But this contrast-gain mechanism may not provide an effective strategy for dealing with prolonged contrast reduction.

To understand why prolonged contrast deprivation might involve a different mechanism from short-term contrast adaptation, consider a simplified characterization as follows. Assume that:

1. the response mechanism (neuron or BOLD) has a limited response range (see Footnote 1) with a maximum value of  $R_{\max}$ ;
2. this finite range of response is mapped onto a wide range of contrast values from 0 to some maximum value,  $C_{\max}$ .

<sup>1</sup>It may be helpful to think of this limited range of response as consisting of finite discrete steps (the assumption of finite steps corresponds to finite steps in neural response associated with discriminable steps in sensation, i.e., "just noticeable differences"). When the upper bound on input contrast is permanently reduced, the discrete set of response steps covers a smaller range of contrast values, resulting in more response steps per unit change in contrast. In other words, a response J.N.D. is associated with a smaller increment in contrast. This is one way of conceiving of "response gain."

This mapping is now referred to as the “contrast response function,” CRF.

This nonlinear system has two competing goals: first, to retain some responsiveness across the entire contrast range; and second, to maximize differential response (i.e., discrimination) near the mean contrast level,  $C_0$ . One prominent property of this nonlinear mapping is that the CRF allocates more of the response range to a narrow band of contrast near the mean contrast  $C_0$ , at the expense of coarser response coding for contrast levels much lower or higher than the mean. In other words, the derivative of the CRF is highest near  $C_0$  and decreases for contrast levels at increasing multiplicative differences above or below  $C_0$ .

Now consider how such a system might respond in situations of short-term and long-term contrast adaptation: 1) *Short-term adaptation is a situation in which there is a change in mean contrast,  $C_0$ , but the overall contrast range (0 to  $C_{max}$ ) remains unchanged.* In this case, the system simply moves the steeper part of the CRF to center on the new value of  $C_0$ . This is what is termed the “contrast gain” model. On a response vs. log contrast scale, the CRF shifts leftward or rightward to re-center the most sensitive part of the curve (i.e., highest derivative) near  $C_0$  (Figure 1B). But the CRF continues to cover the entire contrast range from 0 to  $C_{max}$ . If the mean contrast  $C_0$  decreases, the CRF shifts to the left on the log contrast scale of the CRF. The corresponding effect on the TvC function is a diagonal shift downward and to the left in log-log coordinates (dashed line in Figure 1A); 2) *Long-term adaptation to reduced contrast is a situation in which the mean contrast  $C_0$  may stay constant, but the maximum contrast  $C_{max}$  is reduced substantially, e.g., by a factor of 5.* In this case, because the overall contrast range is reduced, the system can allocate more of its limited dynamic range to the narrow band of contrast values around  $C_0$ . The effect is to steepen the CRF near  $C_0$  (Figure 1C). This is what is termed the “response gain” model. On a response vs. log contrast scale, the CRF has a reduced contrast range (because  $C_{max}$  is smaller), but the CRF is steeper (higher derivative) at  $C_0$ . But again the CRF continues to cover the entire contrast range from 0 to  $C_{max}$ . The corresponding change in the TvC is expected to be a vertical downward shift representing improved contrast discrimination across the range of testable pedestal contrasts (solid line in Figure 1A).

The above analysis implies that we would expect contrast gain to describe short-term “adaptation” for a system that retains a wide range of contrast inputs but is currently dominated by a specific input contrast  $C_0$ . We would expect response gain to describe CRF changes in a system that is confronted with a long-range reduction in the overall contrast range designated by  $C_{max}$ .

### Linking psychophysical contrast discrimination and fMRI BOLD contrast response

The third goal of this study was to confirm the theoretical linkage between TvC and CRF. Earlier studies have shown good agreement between TvCs and CRFs measured in V1 with fMRI (Boynton, Demb, Glover, & Heeger, 1999; Zenger-Landolt & Heeger, 2003) such that the TvC is approximately proportional to 1 over the derivative of the CRF (see Equation 4 in Linking psychophysics and fMRI BOLD measurements section). We focused on the early visual areas V1 and V2 for three reasons:

1. There is already evidence linking the CRFs measured with fMRI BOLD signals to psychophysical contrast discrimination data (e.g., Boynton et al., 1999);
2. Higher-level cortical areas such as hV4 and Lateral Occipital Complex (LOC) do not appear to represent contrast faithfully (e.g., Gardner et al., 2005; Murray & He, 2006); and
3. With grating stimuli, BOLD signals can be measured more reliably in early visual areas, increasing the likelihood of finding subtle adaptation effects.

In summary, our empirical predictions are that adaptation will produce:

1. a decrease in contrast discrimination thresholds compared with pre-adapted thresholds;
2. an increase in the gain of fMRI contrast response functions; and
3. a reduction in contrast discrimination thresholds for the unadapted fellow eye.

Confirmation of these predictions would lend support to the compensation hypothesis, and would indicate that the adaptation effects are cortical in origin.

## METHOD

### Apparatus

We used artificial contrast reduction to test normally sighted subjects. Contrast reduction was implemented using a disk-shaped (36 mm in diameter) contrast-reducing filter worn in front of the eye. The filter attenuated contrast by a factor of 3 (0.5 log unit) while minimizing blur (acuity reduction is less than 0.2 logMAR unit). The filter also has a factor of 2 (0.3 log unit) luminance reduction. The filter is one of a series of contrast filters built by Denis Pelli for research purposes (c.f., Pelli, 1987, pp. 134–146) using 0.5  $\mu\text{m}$  diamonds and clear casting acrylic. The contrast reduction factor was controlled by making filters with various concentrations of diamonds (Pelli, personal communication, September 22, 2006). The filters were calibrated psychophysically by measuring contrast sensitivity (Pelli-Robson test) with and without the filter in front of the eye (Table 1). We further confirmed the filter's contrast reduction by comparing the contrast-detection thresholds for the grating patterns used in the Main experiment, for viewing with the contrast-reducing goggles and the luminance matched Neutral Density (ND)-filter goggles. As expected, we observed a three-fold elevation of contrast-detection threshold for the contrast-reducing goggles viewing condition (mean ratio across three subjects of  $3.13 \pm 0.19$ ).

The filter's blur was also calibrated psychophysically by measuring visual acuity (Lighthouse Distance acuity test) with and without the filter in front of the eye (Table 1). The luminance attenuation of the filter was calibrated with a MINOLTA CS-100 Chroma Meter.

Two types of goggles were used for this study. For one set of goggles, the contrast-reducing filter was worn over the subject's dominant eye, with dominance determined by a subjective alignment test. A translucent occluder, transmitting virtually no pattern information, but matched for overall light transmission, covered the fellow eye. The filter and occluder were mounted in goggles which blocked all light except through the filter apertures. We refer to these goggles as contrast-reducing goggles. For the second set of goggles, a neutral density (ND) filter (optical density = 0.3 log units), matched for luminance attenuation with the contrast-reducing filter, was worn over the dominant eye and the translucent occluder was mounted over the fellow eye. We refer to these goggles as ND-filter goggles.

### Subjects

Three subjects participated in this study. All subjects had normal or corrected-to-normal vision, and had normal contrast sensitivity (Table 1). They were experienced psychophysical subjects (three of the authors) and served in both behavioral and fMRI experiments. Written informed consent was obtained in accordance with a protocol approved by the University of Minnesota Institutional Review Board.

### Experimental design

This study consisted of three experiments (Main, Control and Interocular-transfer tests). The main experiment examined the effect of prolonged contrast attenuation on contrast coding.

Separate days were devoted to the effects of adaptation on behavior (psychophysics) and brain response (BOLD). In both cases, subjects wore the contrast-reducing goggles during pre- and post tests, as well as during the four hours of adaptation (Figure 2).

During the four hours of goggles adaptation, subjects went about their usual daily activities such as reading, working on computers, walking around the building, and eating lunch. We selected four hours of adaptation because pilot testing with two hours revealed effects that were weaker and hard to measure.

A control experiment was identical to the main experiment except that subjects wore the ND-filter goggles, with no contrast attenuation, during the 4-hour adapting period. Finally, to examine interocular transfer, subjects had four hours of adaptation with the contrast filter over one eye and the translucent occluder over the other eye as in the main experiment. But the pre- and post tests were conducted on the unadapted fellow eye, that is, the eye that wore the translucent occluder during the adapting period. During the pre- and post testing, the unadapted eye viewed the stimulus through the contrast-reducing filter.

In summary, in all three experiments the pre- and post tests for both behavioral and fMRI measurements were conducted while subjects wore the contrast-reducing goggles. The difference between the main and control experiments lies in whether subjects wore the contrast-reducing goggles (main experiment) or ND-filter goggles (control experiment) during the adapting period. The difference between the main and interocular-transfer experiments is whether the adapting eye was tested or the unadapted fellow eye was tested.

### Behavioral measurement

**Stimuli**—The test stimulus was a vertical 2 cycles per degree (cpd) sinusoidal grating placed in an annulus (inner radius, 2°; outer radius 9°, see Figure 3). The edges of the annulus were smoothed using a Gaussian kernel with standard deviation ( $\sigma$ ) of 1°. A peripheral annulus grating was used rather than a full-field grating for compatibility with fMRI testing. The stimulus contrast is expressed as Michelson contrast, which is defined as the ratio:

$$C = (L_{max} - L_{min}) / (L_{max} + L_{min}), \quad (1)$$

where  $L_{max}$  and  $L_{min}$  are the peak and minimum luminance of the stimulus respectively. Stimuli were displayed on a uniform gray field (46 cd/m<sup>2</sup>) at a viewing distance of 55 cm. The stimuli were generated and controlled using Matlab (version 7.0) and Psychophysics Toolbox extensions (Mac OS X) (Brainard, 1997; Pelli, 1997), running on a Power Mac G5 computer (model: M73). The display was a SONY Trinitron color graphic display (model: GDM-FW520; refresh rate: 85 Hz; resolution: 1024 × 768). Stimuli were rendered with a video card with 8 bit input resolution and 14 bit output resolution using Cambridge Research System Bits++. Luminance of the display monitor was linearized using an 8-bit look-up table in conjunction with photometric readings from the colorCAL colorimeter (Cambridge Research System). The chromaticity of the monitor was also made linear so that the RGB values could be uniformly distributed across all grayscale levels.

**Procedure**—Contrast increment thresholds were measured with a temporal two-alternative forced-choice (2AFC) staircase procedure. Seven pedestal levels (0%, 0.3%, 1%, 1.6%, 3.3%, 8.3% and 16.6% filtered contrast (see Footnote 2)) were tested and the step size of the staircase was 1 dB. A 3-down-1-up staircase rule was adopted yielding a threshold criterion of 79.4%

<sup>2</sup>The filtered contrast denotes the stimulus contrast taking into account attenuation by the contrast-reducing goggles. It was obtained by dividing the stimulus contrast by a factor of 3.

correct (Wetherill & Levitt, 1965). The geometric mean of 7 staircase reversals was taken as the contrast threshold for each staircase run. The final thresholds were based on a geometric mean of four thresholds obtained from repeated measures on two different days. The order of pedestal contrasts was counterbalanced with ascending and descending sequences on both days.

In a discrimination trial, the stimuli  $C$  and  $C + \Delta C$  were each presented for 200 ms, accompanied by an auditory tone, and separated by 500 ms (Figure 3).

The subjects' task was to judge which stimulus interval contained the higher contrast by pressing one of two keys. Auditory feedback was given whenever a wrong answer was made. Subjects were given a series of practice trials before the experimental test. A small cross in the center of the stimulus served as a fixation mark to minimize eye-movements throughout the experiment. A chin-rest was also used to minimize head movements. Contrast-discrimination thresholds were measured in pre- and post-tests. Each subject participated in 5 separate sessions of behavioral testing on five different days: four sessions were dedicated to the experimental conditions (two for the main experiment and two for the interocular transfer experiment) and one session for the control experiment.

### fMRI measurement

**Stimuli**—The test stimuli were the same as those in the psychophysical experiments, except that the stimuli were counterphase flickered at 10 Hz. The annulus grating was chosen because it is difficult to identify the boundaries between the early visual cortical areas for the central part of the visual field. The display was controlled and generated by a DELL Laptop computer running MATLAB (version. 6.2) with PsychToolBox extensions (Windows 2000) (Brainard, 1997; Pelli, 1997). In the scanner, the stimuli were back-projected using a video projector (60 Hz) onto a translucent screen placed inside the scanner bore. Subjects viewed the stimuli through a mirror located above their eyes. The viewing distance was 85 cm. The stimulus was displayed on a uniform gray field ( $90 \text{ cd/m}^2$ ). The luminance of the display projector was made linear using an 8-bit look-up table with photometric readings from a MINOLTA CS-100 Chroma Meter.

**Procedure**—fMRI BOLD contrast response functions were measured in pre- and post-tests. The stimulus contrasts were determined by the results from the behavioral data, so that the fMRI contrast response function would include the stimulus contrast corresponding to the dipper portion of the contrast-discrimination function. Since subjects reach the dipper at a pedestal stimulus contrast of 1% with the contrast-reducing goggles, we used four stimulus contrast levels (1%, 3.3%, 8.3%, 16.6% filtered contrast).

The four contrast stimulus conditions were measured in separate scans, and the set of contrasts was repeated twice, one in ascending and the other in descending order. Thus, 8 scans were performed in one session. Each subject participated in 9 separate sessions—one to define retinotopic areas, two pre- and two post tests for the main experiment, and two pre- and two post-tests for the control experiment. The contrast response functions for the target contrast were measured using a block design paradigm, in which 12 sec test blocks and 18 sec baseline blocks were interleaved (Figure 4A). Each scan consisted of an initial 10 sec that was discarded, followed by an 18 sec off-period and then seven on- and off-periods (each 30 sec), which made the duration of each scan 238 sec (approximately 4 min).

To equate for attentional demand, we measured subjects' contrast response functions while they did a moderately demanding fixation task, rather than doing the contrast discrimination task. During scanning, the fixation point changed to a cross (either vertical or 45 degree tilted) every 2 sec. The cross lasted 400 ms, then changed back to the fixation point. Subjects were



asked to press one of the two buttons to indicate the orientation of the cross. Subjects performed this fixation task throughout the scanning period (i.e., for both stimulus and blank intervals). Subjects were given a series of practice trials outside the scanner.

We followed the standard retinotopic mapping method (Engel, Glover, & Wandell, 1997; Sereno et al., 1995). Rotating wedge scans served to map boundaries between visual areas and expanding ring scans served to map the visual representations at different eccentricities. Each scan of annuli and wedge lasted 190 sec and 286 sec respectively. An independent scan was used to define the regions of interest (ROI). Subjects passively viewed images of a contrast-reversing (10 Hz) high-contrast sine grating annulus (inner radius 2°; outer radius 9°) centered at fixation. The grating annulus was presented in 20 sec stimulus blocks, interleaved with 20 sec blank blocks. Each block type was repeated 5 times in the scan, which lasted 200 sec.

**fMRI data acquisition**—The fMRI data were collected using a 3-Tesla Siemens Trio scanner with an 8-channel head coil. Images were collected using a T<sub>2</sub>\*-weighted echo planar sequence: echo time (TE), 30 ms; repetition time (TR), 2000 ms; flip angle, 60°; field of view (FOV), 192 × 192 mm<sup>2</sup>; matrix: 64 × 64, slice thickness: 3 mm, gap: 0 mm, number of slices: 28, slice orientation: axial. The bottom slice was positioned at the bottom of the temporal lobes. A high-resolution 3D structural data set (3D MPRAGE; 1 × 1 × 1 mm<sup>3</sup> resolution) were collected in the same session before the functional runs.

**fMRI data analysis**—The anatomical volume for each subject in the retinotopic mapping session was inflated using BrainVoyager 2000. Functional volumes in all the sessions for each subject were preprocessed including 3D motion correction using SPM99, linear trend removal, and high-pass (0.015 Hz) (Smith et al., 1999) filtering using BrainVoyager 2000. The images were then aligned to the anatomical volume in the retinotopic mapping session and transformed into Talairach space. The first 10 sec of BOLD signals were discarded to minimize transient magnetic saturation effects. All analyses were performed on an individual subject basis.

A general linear model procedure was used for region of interest (ROI) analysis. The ROIs in V1 and V2 were defined as areas that responded more strongly to the flickering annulus than blank interval ( $p < 0.0001$ , uncorrected), constrained by the retinotopic maps. For each fMRI scan, the time course of MR signal intensity was first extracted by averaging the data across all the voxels within the pre-defined ROI, and then normalized by the average of the last two time points, just preceding the stimulus onset, of all 18 sec blank intervals. The response level in a ROI was extracted by averaging the response within a 6–12 sec interval after the start of the stimulus block, and then averaged according to different contrast conditions.

### Linking psychophysics and fMRI BOLD measurements

The following equation (e.g., Boynton et al., 1999; Naka & Rushton, 1966; Ross & Speed, 1991) was used to fit fMRI BOLD contrast response functions.

$$R = R_{\max} (C^{n+m}) / (C^n + C_{50}^n), \quad (2)$$

where  $R$  is the response,  $R_{\max}$  is the maximum response,  $C$  is stimulus contrast,  $C_{50}$  is the semi-saturation constant. For low contrasts ( $C < C_{50}$ ), the function behaves like a power function with an exponent of  $n + m$ . For high contrasts ( $C > C_{50}$ ), the function behaves like a power function with an exponent of  $m$ . The typical values of  $n$  and  $m$  are 2 and 0.4 respectively, so that the function is expansive ( $C^{2.4}$ ) at low contrasts and compressive at high contrasts ( $C^{0.4}$ ) (Legge & Foley, 1980).

The fits were achieved using a simplex search method (Lagarias, Reeds, Wright, & Wright, 1998) to search for the optimal fit producing the least squares error. Psychophysical contrast increment thresholds can be predicted from a CRF (Equation 2) by assuming that a contrast increment is detectable when the response  $R$  increases by a criterion amount (Legge & Foley, 1980). That is, the predicted threshold,  $\Delta C$  satisfies:

$$R(C+\Delta C) - R(C) = \Delta R_c, \quad (3)$$

where  $\Delta C$  is the threshold contrast increment and  $\Delta R_c$  is the criterion response increment. Equation 3 can be solved numerically for various pedestal contrast  $C$  to produce a predicted TvC curve (see details in Boynton et al., 1999). As a result, the TvC curve is approximately proportional to 1 over the derivative of the CRF:

$$\Delta C = \Delta R_c (1/dR/dC), \quad (4)$$

Then, Equation 4 is fit to the TvC functions. The shape of the TvC is determined by the relative values of  $C_{50}$ ,  $n$  and  $m$ . The criterion response increment  $\Delta R_c$ , acts as a scaling factor of the TvC curve so that changing  $\Delta R_c$  shifts the TvC curve vertically on the log-log coordinates. The predicted  $\Delta C$  increases with pedestal contrast for high contrasts ( $C > C_{50}$ ) where the CRF is compressive. The predicted  $\Delta C$  decreases with increasing pedestal contrast for low contrasts ( $C < C_{50}$ ) where the CRF is accelerating.

Simultaneous fits to the TvC and fMRI BOLD CRF data were achieved for each subject using the simplex search method to minimize the weighted residual sum of squares. The reciprocal of the variance of each data set (the TvC and CRF) were used as weights (i.e.,  $1/\sigma^2$ ). The weights were incorporated into the least squares criterion of the simultaneous fits so that the two types of data (the TvC and CRF) would contribute approximately equally in the curve fitting (c.f., Boynton et al., 1999).

## RESULTS

### Subjective reports

At first, subjects found that performing daily activities with the contrast-reducing goggles, such as reading and walking around, to be physically and mentally demanding. However, they reported that after about three hours, they had become less consciously aware of the presence of the goggles. Paraphrasing some of their comments, "At first, I had difficulty finding my way around the building, in particular the stairs. Also, accurate typing for routine computer work was difficult and reading hard copy was also relatively challenging. However, these difficulties gradually diminished. Those tasks did not seem to be as difficult at the end of the adaptation."

One subject also commented that "In the pre-test, I hardly saw any stimulus grating at low contrast levels, but after 4 hours adaptation, in the post-test, those stimuli became noticeably visible and less murky".

These subjective descriptions suggest that there might be some compensatory changes in subjects' perceived contrast as a result of wearing the contrast-reducing goggles.

### Linkage between TvCs and fMRI CRFs

The TvC and CRF data sets for comparable conditions from individual subjects were fit simultaneously using the four parameters ( $R_{\max}$ ,  $C_{50}$ ,  $n$ ,  $m$ ) in Equation 2. Fits to both TvC and CRF shared the four parameters. Then the criterion response value,  $\Delta R_c$ , allowed contrast



increment thresholds to be predicted from CRFs using Equation 4. Thus, five parameters varied freely in the fitting.

The simultaneous fits were performed on each data set from four different conditions (i.e., pre- and post-test conditions with contrast-reducing goggles and neutral-density goggles). Figure 5 shows an example of the results for the group average for the TvC data and the CRF data from cortical areas V1 and V2 respectively. The contrast increment thresholds were plotted as a function of pedestal contrast in log-log coordinates (Figure 5A), demonstrating the characteristic dipper shape (e.g., Legge, 1981). The fMRI BOLD signal changes (%) were plotted as a function of stimulus contrast in linear-log coordinates (Figures 5B and 5C). The fMRI BOLD signals increased with increasing stimulus contrast in both V1 and V2 areas, consistent with earlier studies (Boynton et al., 1999; Gardner et al., 2005; Olman, Ugurbil, Schrater, & Kersten, 2004; Zenger-Landolt & Heeger, 2003).

The smooth curves in Figure 5 show examples of simultaneous fits to both TvC and CRF for the pre-test in the main experiment. The fits pass through nearly all data points, demonstrating that the underlying model linking the fMRI and behavioral data captures the two data sets well.

To examine whether the simultaneous fit is statistically as good as separate fits to the TvC and CRF data, we performed the nested model test (see Footnote 3) on two competing models (i.e., the full vs. reduced models) with the following steps:

1. For the full model (i.e., separate fit), the model equation (Equation 2) was fit separately to the TvC and the CRF in the cortical region of V1, i.e., the values of all four parameters ( $R_{\max}$ ,  $C_{50}$ ,  $n$ ,  $m$ ) of Equation 2 were permitted to change independently between the TvC and CRF. Thus, the full model has eight free parameters;
2. The reduced model, the model equation (Equation 2) was fit simultaneously to both the TvC data and the CRF data, i.e., the four parameter values are identical for both TvC and CRF. Thus, the reduced model has five free parameters including  $\Delta R_c$ ;
3. Then, the residual sums of squares (*RSS*) of the full and reduced models were compared to see if the variance accounted for by the added parameters in the full model is significantly larger than expected by chance:
4. We repeated steps 1–3 for the TvC and the CRF in the cortical region of V2.

The nested model test (i.e., *F*-test) confirmed that the reduced model (simultaneous fit) is as good as the full model (separate fits) for all the experimental conditions ( $p \gg 0.05$ ).

This is true whether the fMRI data are from cortical regions V1 or V2. In other words, the simultaneous fit provides the simplest and best account for both TvC and CRF data. The satisfactory nature of the simultaneous fits provides strong confirmation of the hypothesis, encapsulated by Equation 4, linking fMRI BOLD responses in V1 and V2 to psychophysical contrast-discrimination thresholds. Throughout the rest of this paper, we will rely on this method of simultaneously fitting brain-imaging and behavioral data.

<sup>3</sup>The nested model test (i.e., *F*-test) is to compare competing models, in which one model is nested within another (Cook & Weisberg, 1999). Two models are nested if both contain the same terms and one has at least one additional term. A model with more terms is the full model (equivalently the null hypothesis) and one with lesser terms is the reduced model (i.e., nested or equivalently the alternative hypothesis). If the full model provides a much better fit than does the reduced model, we would expect that the residual sum of squares (*RSS*) under the full model will be considerably smaller than the *RSS* under the reduced model. This comparison provides the basis for a test of the competing models. The test statistics is:  $F_{stat} = ((RSS_{reduced} - RSS_{full}) / (df_{reduced} - df_{full})) / (RSS_{full} / df_{full})$  where  $RSS_{full}$  is the sum of squares under the full model and  $RSS_{reduced}$  is the sum of squares under the reduced model. When the null hypothesis is true, this statistic has an  $F_{d1, d2}$  distribution with  $d1 = df_{reduced} - df_{full}$  and  $d2 = df_{full}$ . The *p*-value of the test is computed as the probability that an  $F_{d1, d2}$  random variable is as large or larger than the observed value of *F*. In other words, the test evaluates whether the variance accounted for by the added terms in the full model is significantly larger than expected by chance. Using a lattice of nested model, we can select the simplest model which can account best for the data.

Mean parameter values, averaged across three subjects for the best simultaneous fits and their standard errors are listed in Table 2. These parameter values are similar across all the experimental conditions (i.e., main, control, pre- and post-test conditions) except the parameter,  $R_{\max}$  which is affected by adaptation (see Identifying mechanisms of the adaptation effect section). The values provided in Table 2 are taken from the pre-test of the main experiment.

### Effect of adaptation on TvCs and CRFs

We hypothesized that prolonged contrast adaptation would produce decreased contrast discrimination thresholds and increased gain of fMRI contrast responses in the early visual cortical areas (V1 and V2). Consistent with our prediction, we observed both significant decreases in discrimination thresholds and increases in fMRI BOLD CRFs in the post-tests.

The effect of adaptation on contrast discrimination was quantified as  $(pre \log\_threshold) - (post \log\_threshold)$ , and on fMRI response as  $(post \text{ fMRI BOLD response}) - (pre \text{ fMRI BOLD response})$ . If there is no change in either thresholds or BOLD responses between pre- and post-tests, the difference values would be zero. If there is any compensatory change after adaptation, the difference values would be greater than zero (positive sign).

Figure 6 shows average difference values for the main experiment (first column) and control experiment (second column). The horizontal dashed line in each graph represents the value of zero which indicates no change in thresholds or BOLD responses. It is evident that both TvCs and CRFs from the main experiment show mostly upward bars, i.e., compensatory changes while data from the control experiment show minimal changes.

The noticeable downward bars (i.e., elevated thresholds) observed in the control experiment may have been due to fatigue. All the subjects reported some fatigue after wearing the goggles for four hours.

We performed an analysis of variance (ANOVA) on the contrast-discrimination thresholds—2 (test condition: pre vs. post)  $\times$  7 (contrast) repeated measures ANOVA with test condition and contrast as within-subject factors. There was a significant main effect of test condition on discrimination threshold ( $F_{(1,12)} = 31.22, p < 0.01$ ). The results show that discrimination thresholds decrease by an average of  $0.12 \pm 0.04$  log units in the post-tests. There was a significant main effect of contrast ( $F_{(6,12)} = 171.34, p < 0.01$ ), demonstrating the dependency of discrimination thresholds on pedestal contrast. There was no significant interaction between test condition and contrast ( $p = 0.44$ ).

The results of ANOVA from the control experiment revealed neither a significant main effect of test condition nor a contrast by test-condition interaction (all  $p > 0.11$ ), but only the expected significant main effect of contrast on threshold ( $F_{(6,12)} = 74.76, p < 0.01$ ). We also conducted an ANOVA on the fMRI contrast response—2 (test condition: pre vs. post)  $\times$  4 (contrast)  $\times$  2 (area: V1 and V2) repeated measures ANOVA with test condition, contrast and area as within-subject factors. There were significant main effects of test condition ( $F_{(1,22)} = 26.68, p < 0.01$ ). In the post-test, the fMRI contrast response in V1 and V2 areas of the brain were increased on average by a factor of 1.96 and 1.30 respectively. But, neither significant main effects of area nor its interaction with test condition was found (all  $p > 0.63$ ). There were also significant main effects of contrast ( $F_{(3,22)} = 125.42, p < 0.01$ ), indicating the dependence of the fMRI response on contrast level. Significant interaction between test condition and contrast was also found ( $F_{(3,22)} = 7.02, p < 0.01$ ). In the control experiment, we did not observe any significant main effect of test condition, area nor test condition by contrast interaction effect (all  $p > 0.40$ ). Only a significant main effect of contrast on threshold was observed ( $F_{(3,22)} = 111.45, p < 0.01$ ).

### Fixation orientation task in the scanner

Subjects' CRFs were measured while they were doing a fixation orientation task demanding attention (see details in Method section). Our results show that subjects' performance on the fixation task stayed nearly constant across different conditions: mean accuracy collapsed across contrast levels was  $85 \pm 7\%$  for pre-test and  $87 \pm 10\%$  for post-test in the main experiment;  $84 \pm 8\%$  for pre-test and  $80 \pm 13\%$  for post-test in the control condition.

A 2 (test condition: pre vs. post)  $\times$  4 (contrast) repeated measures ANOVA with test condition and contrast as within-subject factors was conducted on fixation orientation performance. For both main and control experiments, we did not observe any significant main effect of test condition, contrast nor test condition by contrast interaction effect (all  $p > 0.13$ ).

These results help us to rule out changes in attentional modulation as an explanation for the increase in cortical contrast response following adaptation.

### Identifying mechanisms of the adaptation effect

Figure 7A shows contrast increment thresholds, averaged across subjects, plotted as a function of filtered pedestal contrast in log-log coordinates. Figures 7B and 7C show fMRI BOLD signal changes (%) in V1 and V2, averaged across subjects, as a function of filtered stimulus contrast in linear-log coordinates. The patterns of results from individual subjects were similar. We used the simultaneous fit to TvC and CRF data (see Linkage between TvCs and fMRI CRFs section) to identify the mechanism underlying the adaptation effect.

We did so by examining the parameter changes in Equation 2 and interpreted these changes to distinguish between contrast gain and response gain: an increase of  $R_{\max}$  in the post-test signifies response gain; a decrease of  $C_{50}$  signifies contrast gain.

Changes in the parameters were studied with the nested model test (see Footnote 3) with a lattice of six models (the full and reduced models, and four intermediates). The nested model test is often used to identify the model that best accounts for the given data with the fewest parameters (c.f., Li, Lu, Tjan, Doshier, & Chu, 2008). We used the following procedure: in the full model, all four parameters of the model Equation 2 (i.e.,  $R_{\max}$ ,  $C_{50}$ ,  $n$ ,  $m$ ) are changed between the pre- and post-test conditions. That is, there are eight free parameters in the model. In the reduced model, the pre- and post-test conditions share all four parameters of the model equation. Thus, there are four free parameters in the reduced model. In intermediate models, some but not all four parameter values are shared between pre- and post-test conditions. For instance, the  $R_{\max}$  is forced to be identical for the pre- and post-test conditions while other parameters are allowed to vary. Note that the fixed parameter values between pre- and post-test conditions are allowed to vary in the optimization method.

In a nutshell, the response-gain model is the one where only  $R_{\max}$  is allowed to vary between pre- and post-test but the other parameters are forced to have the same values. The contrast-gain model is defined as the one in which only  $C_{50}$  is allowed to vary between pre- and post-test with others being identical. The  $n$ - $m$  model is one with only  $n$  and  $m$  parameters being allowed to vary between pre- and post-test.

The nested model test showed that the best fitting model is the response-gain. The model, shown as smooth curves in Figure 7, accounts for 75.39% (V1) and 74.29% (V2) of the variance in the data. This model is statistically superior to the reduced model ( $F_{(2,20)} = 30.64$ ,  $p < 0.01$ ;  $F_{(2,20)} = 28.90$ ,  $p < 0.01$  for V1 and V2 respectively), and as good as the full model ( $F_{(6,14)} = 0.95$ ,  $p = 0.30$ ;  $F_{(6,14)} = 1.04$ ,  $p = 0.24$ ). In comparison, neither the contrast-gain model nor  $n$ - $m$  model is significantly different from the reduced model (all  $p > 0.1$ ). Both are significantly inferior to the full model, as are the intermediate model that includes  $R_{\max}$  (all  $p < 0.01$ ).

To evaluate the effect of individual differences on model selection, a statistical bootstrap procedure was performed with the following steps:

1. Sampling with replacement a set of TvC and CRF (either V1 or V2) of both pre- and post-test conditions from three subjects;
2. Averaging the re-sampled TvCs and CRFs ( $n = 3$ ), separately for pre- and post-test conditions;
3. Six variants (i.e., a lattice of six nested models as stated above) of the model Equation 2 was fitted simultaneously to both TvC and CRF. Then the residual sum of squares (RSS) of each model was recorded for the nested model test;
4. Using the nested model test, the best fitting model, the one that is not statistically different from the full model but superior to all its reduced models, was selected;
5. The frequency of being chosen as the best fitting model for the six candidate models and their parameter values were recorded;
6. Steps 1–5 were repeated 100,000 times;
7. The mean parameter values and its standard errors of the best fitting model were computed as shown in Table 3.

The bootstrap analysis showed that the response gain model was the best fitting model 96.13% of the time. Neither the contrast gain nor  $n$ - $m$  model was ever the best fitting model. These results support the response-gain model as the best account of our data.

The parameters of the best fitting response-gain model and their standard errors are summarized in Table 3. Adaptation increased  $R_{\max}$  by a factor of approximately 1.30 in units of percent signal changes in V1 and V2 areas.

### Interocular transfer of the adaptation effect

If contrast adaptation occurs at the cortical level where binocular convergence occurs, we would predict an interocular-transfer of the adaptation effect when we measure performance in the occluded eye. However, if the adaptation is pre-cortical (e.g., in the retina or LGN), we would not expect to observe transfer of adaptation to the unadapted occluded eye.

As expected for the cortical site of adaptation, we observed a significant improvement in discrimination sensitivity in the occluded eye following adaptation for all three subjects (Figure 8). The contrast-discrimination results revealed full interocular transfer of the adaptation effect. Discrimination thresholds decreased by an average of  $0.14 \pm 0.01$  log units in the post-tests for the occluded eye, close to the average decrease of 0.12 log units for the adapted eye. A 2 (test condition: pre vs. post)  $\times$  7 (contrast) repeated measures ANOVA revealed that the difference in thresholds between pre- and post-tests was significant ( $F_{(1,12)} = 39.46, p < 0.01$ ). The difference in thresholds across contrast levels was also significant ( $F_{(6,12)} = 153.90, p < 0.01$ ), demonstrating the dependency of discrimination thresholds on pedestal contrast. No significant interaction effect was found ( $p > 0.1$ ).

Our transfer test does not rule out the possibility that monocular occlusion (i.e., adaptation to a field with zero contrast) produces the adaptation effect. This would not be expected, however, if the visual system is adapting in a compensatory way to a change in the contrast characteristics of visible patterns.

## DISCUSSION

Our major finding is that four hours of exposure to a low-contrast visual environment produced significant changes in contrast coding demonstrated both behaviorally and in cortical responses. The nature of the changes was consistent with our three predictions from the compensation hypothesis:

1. improvement in contrast-discrimination sensitivity;
2. an increase in the gain of fMRI contrast response functions in visual cortical areas V1 and V2, and
3. interocular transfer of these adaptation effects.

The mechanisms of this adaptive change can be accounted for by the response-gain model. In addition, we also established quantitatively the adequacy of a simple linking hypothesis relating neural response to behavioral contrast-discrimination data (Boynton et al., 1999; Legge & Foley, 1980; Zenger-Landolt & Heeger, 2003).

### Linking psychophysical TvC to fMRI BOLD CRF

Our results confirmed the theoretical linkage between TvC and CRF, that is, an increment in contrast ( $\Delta C$ ) can be detected by a human observer only when the increment in the neuronal response increases by some criterion amount ( $\Delta R_c$ ) (Legge & Foley, 1980; Ross & Speed, 1991). The hypothetical relationship between psychophysical TvCs and CRFs measured with fMRI has been demonstrated in early human visual cortical areas (e.g., Boynton et al., 1999; Zenger-Landolt & Heeger, 2003). However, our study is the first to show that the linkage is retained following a manipulation that is likely to modify contrast coding.

Previous psychophysical estimates of the underlying CRF have a typical value of approximately 0.4 for the exponent in the compressive region (Foley & Legge, 1981; Legge & Foley, 1980). Boynton et al. (1999) obtained a value of 0.3 for the exponent in their fMRI study. Our best-fit parameter value has an exponent,  $m \approx 0.5$  in the compressive region, which is comparable to those of previous studies.

Psychophysical estimates of the underlying CRFs suggest an expansive region with an exponent of about 2.4–2.7 (Foley, 1994; Legge & Foley, 1980). Boynton et al. (1999) observed an exponent of about 1.6 in the expansive region. The corresponding value from our study for  $n + m \approx 4$  which is significantly larger than the values observed in earlier studies. This result corresponds to a more pronounced dip in the TvC function at near threshold contrast than usually observed.

Boynton et al. (1999) showed that the estimate of  $\Delta R_c$  is about 0.02 in units of a percentage change in BOLD signals, meaning that two stimuli producing fMRI BOLD responses that differ by this amount will be distinguishable behaviorally approximately 79% of the time, regardless of the pedestal contrast. Our best-fit parameter value of  $\Delta R_c$  is about 0.06 which is larger than the value found by Boynton et al. (1999).

Boynton et al. (1999) used a contrast discrimination task in the scanner. We used a fixation orientation task with passive viewing of contrast in order to minimize top-down effects from attention. Some of the discrepancies in parameter values between ours and Boynton's study might be accounted for by methodological differences including task differences influencing attention.

Our best-fit parameter values for the simultaneous fit to both TvCs and CRFs are very similar across V1 and V2 areas, suggesting similar contrast coding. These results are consistent with

Gardner et al. (2005)'s findings, demonstrating similar contrast gain in V1 through V3 areas following short-term adaptation.

Whether the adaptive changes observed in the early visual areas are generalized to higher cortical areas is of importance, but little is known. Only two studies have addressed contrast adaptation in higher areas: monkey MT (Kohn & Movshon, 2003) and hV4 (Gardner et al., 2005). Perhaps, as suggested by Kohn and Movshon (2003), contrast adaptation occurs mostly in the early visual area V1 and then is simply passed along to later stages of the system, rather than taking place independently in different areas. However, we cannot rule out some possible feedback mechanism from higher level areas as hinted at by Gardner et al. (2005).

### Compensatory changes following contrast deprivation

Our results showed that prolonged exposure to low contrasts lead to compensatory changes in visual contrast coding in both behavioral and physiological domains. We observed that following the prolonged adaptation, discrimination thresholds decreased by an average of  $0.12 \pm 0.04$  log units and the fMRI contrast response in V1 and V2 areas of the brain were increased by average factors of 1.96 and 1.30 respectively.

Nevertheless, it is possible that covert attention could play a role in the observed difference in fMRI contrast response between pre- and post-tests. Perhaps, subjects paid more attention to stimulus contrast in the post-test than pre-test which could have resulted in an increase in cortical contrast responses. It has been reported that attention modulates fMRI contrast response function via additive gain (Buracas & Boynton, 2007; Murray, 2008) or multiplicative gain (Li et al., 2008) of fMRI contrast response functions.

Increased attention to the annular contrast stimuli would be expected to result in decreased performance in the fixation orientation task in central vision. If so, we should be able to observe a noticeable decrease in fixation orientation performance in the post-tests and similarly, differences in fixation performance in the main experiment (pre vs. post) and control experiment (pre vs. post).

We did not find any significant differences between pre- and post tests in performance on the fixation task for either the main or control experimental conditions. These results encourage us to believe that subjects' covert attention is not likely to play a role in the observed increase in cortical contrast response following adaptation.

According to the contrast attenuation model (Rubin & Legge, 1989), there should be a direct correspondence between the input contrast and the perceptual or neural representation of the input contrast. In other words, when the input contrast is reduced by some attenuation factor there should be a corresponding reduction in the perceptual level of the contrast by the same attenuation factor. This model does not anticipate any modification in the visual coding of retinal-image contrast. Our findings however, show that the prolonged exposure to reduced contrast changes the neural representation so that the precision of contrast coding improves for low retinal-image contrasts.

### The mechanism of the adaptation to prolonged contrast deprivation

Our study provides evidence for response gain as the mechanism underlying adaptation to prolonged contrast deprivation. Our results showed adaptation increases the  $R_{\max}$  parameter value by a factor of approximately 1.30 for V1 and V2 areas. Changes in the contrast response function of visual cortical neurons following contrast adaptation are often mathematically formulated as either a contrast gain model or a response gain model (e.g., Albrecht, Farrar, & Hamilton, 1984; Hood, 1978). The contrast gain model is characterized by a lateral shift of the response curve, resulting in changes in the value of the semi-saturation ( $C_{50}$ ) parameter only.



The response gain model is characterized as a vertical shift of the curve, resulting in changes in the value of the maximum response ( $R_{\max}$ ) parameter only.

Short-term contrast adaptation has been studied by having subjects adapt to a certain contrast level for a short time scale (i.e., tens of seconds to ten minutes) and comparing their thresholds (or BOLD response) before and after the adaptation. The mechanism of this relatively short-term contrast adaptation has often been accounted for by a contrast-gain model in which the system adjusts the dynamic range of the CRF to be centered near the mean stimulus contrast. For example, single cell studies in monkey and cat V1 showed that short-term contrast adaptation results in mostly horizontal shifts of contrast response functions (Albrecht et al., 1984; Ohzawa, Sclar, Freeman, 1985; Sclar, Lennie, & DePriest, 1989). This mechanism tends to optimize vision for detecting differences in the contrasts near the prevailing mean contrast in the environment. Human brain imaging (fMRI) and visual evoked potential (VEP) studies have also revealed contrast gain after short-term adaptation in human visual cortex (Bach, Greenlee, & Böhler, 1988; Gardner et al., 2005; Heinrich & Bach, 2001). While not conclusively demonstrating contrast gain, psychophysical studies have also suggested that adaptation enhances contrast sensitivity around the adapting contrast (Abbonizio, Langley, & Clifford, 2002; Greenlee & Heitger, 1988; Pestilli et al., 2007; Ross & Speed, 1991).

Laughlin (1981, 1990) pointed out that the process of contrast adaptation may promote coding efficiency by improving accuracy of contrast coding within the constraints of a limited dynamic response range and intrinsic noise. As discussed in the Introduction, the contrast gain mechanism is appropriate for a system that must cope with changing mean contrast levels within a fixed but wide range of overall contrast levels. The response-gain mechanism seems well designed for a system adapting to a reduced range of overall contrast.

A possible long-term adaptive change in contrast coding has been observed in the vertebrate visual system. Burkhardt, Fahey, and Sikora (2006) studied the contrast response functions of retinal bipolar cells in the Tiger-Salamander. This animal lives in low contrast watery environments. It was found that the dynamic range of the bipolar cell population brackets the distribution of contrasts found in natural images in the salamander's environment, supporting the view that its contrast coding is optimal for its low contrast environment.

Our study is the first to examine changes in contrast coding following long-term contrast reduction. Our findings indicate that the adaptation mechanism differs from the contrast-gain mechanism which accounts for short-term adaptation. Our results provide evidence for a response gain mechanism in which the slope of the CRF is steeper near the prevailing contrast following adaptation.

### **Clinical implications for low-vision**

The question of whether there are any compensatory perceptual or neural changes in response to visual deprivation is relevant to low-vision rehabilitation. One possible implication of our findings is that after prolonged experience with eye conditions yielding reduced retinal-image contrast, such as cataract, people might achieve higher discrimination sensitivity for low contrasts compared to people with normal vision. An analogous effect appears in our results. After adapting to low contrasts, subjects' contrast discrimination thresholds were lower than those of subjects wearing the ND filters at least for a certain range of contrast (i.e., 1%, 1.6% and 3.3%) by up to a factor of 1.60.

It remains to be determined if neural compensation takes the form of response gain for cases of contrast deprivation over months or years. Studies of amblyopia hinted a possible role of neural compensation in chronically deprived visual systems (Hess & Bradley, 1980; Simmers, Bex, & Hess, 2003). Hess and Bradley (1980) reported that despite marked contrast deficits at

threshold, no contrast coding abnormality in amblyopia was found in suprathreshold vision (typical of daily vision). They argued that substantial neural compensation may have occurred within the amblyopic visual system, which in turn may explain why adult amblyopes do not accept that the degraded vision from their amblyopic eye looks like a defocused version of what they see through their fellow normal eye (Hess & Bradley, 1980). Similar neural compensation or adjustment for perceived contrast and blur has been also observed in normal vision (Georgeson & Sullivan, 1975; Webster, Georgeson, & Webster, 2002).

## Conclusions

In summary, our findings are consistent with the *compensation hypothesis*, that prolonged exposure to low contrast stimuli results in compensatory changes in the adult human visual system. We found that prolonged contrast reduction resulted in:

1. improvement in behavioral contrast discrimination;
2. increased fMRI contrast responses in the early visual cortical areas of the brain (V1 and V2); and
3. interocular transfer of the adaptation effect, confirming that the adaptation occurs at the cortical level.

Quantitative analysis of our data provides evidence for response gain as the mechanism underlying changes in contrast coding in the presence of prolonged contrast deprivation.

## ACKNOWLEDGMENTS

We thank Bosco Tjan for his helpful advice on data analysis. We thank Steve Engel for his helpful comments on an earlier draft of the manuscript. We also thank Cheryl Olman, Huseyin Boyaci, and Yi Jiang for useful advice on experimental design. This work was supported by NIH grant R01 EY002934.

## REFERENCES

- Abbonizio G, Langley K, Clifford CW. Contrast adaptation may enhance contrast discrimination. *Spatial Vision* 2002;16:45–58. [PubMed: 12636224]
- Albrecht DG, Farrar SB, Hamilton DB. Spatial contrast adaptation characteristics of neurons recorded in the cat's visual cortex. *The Journal of Physiology* 1984;347:713–739. [PubMed: 6707974]
- Bach M, Greenlee MW, Böhler B. Contrast adaptation can increase visually evoked potential amplitude. *Clinical Vision Science* 1988;3:185–194.
- Boynton GM, Demb JB, Glover GH, Heeger DJ. Neuronal basis of contrast discrimination. *Vision Research* 1999;39:257–269. [PubMed: 10326134]
- Brainard DH. The Psychophysics Toolbox. *Spatial Vision* 1997;10:433–436. [PubMed: 9176952]
- Buracas GT, Boynton GM. The effect of spatial attention on contrast response functions in human visual cortex. *Journal of Neuroscience* 2007;27:93–97. [PubMed: 17202476]
- Burkhardt DA, Fahey PK, Sikora MA. Natural images and contrast encoding in bipolar cells in the retina of the land- and aquatic-phase tiger salamander. *Visual Neuroscience* 2006;23:35–47. [PubMed: 16597349]
- Cook, RD.; Weisberg, S. *Applied regression including computing and graphics*. New York, NY: Wiley Interscience; 1999.
- Engel SA, Glover GH, Wandell BA. Retinotopic organization in human visual cortex and the spatial precision of functional MRI. *Cerebral Cortex* 1997;7:181–192. [PubMed: 9087826]
- Fine I, Smallman HS, Doyle P, MacLeod DI. Visual function before and after the removal of bilateral congenital cataracts in adulthood. *Vision Research* 2002;42:191–210. [PubMed: 11809473]
- Foley JM. Human luminance pattern-vision mechanisms: Masking experiments require a new model. *Journal of Optical Society of America A, Optics, Image Science, and Vision* 1994;11:1710–1719.

- Foley JM, Legge GE. Contrast detection and near-threshold discrimination in human vision. *Vision Research* 1981;21:1041–1053. [PubMed: 7314485]
- Gardner JL, Sun P, Waggoner RA, Ueno K, Tanaka K, Cheng K. Contrast adaptation and representation in human early visual cortex. *Neuron* 2005;47:607–620. [PubMed: 16102542]
- Georgeson MA, Sullivan GD. Contrast constancy: Deblurring in human vision by spatial frequency channels. *The Journal of Physiology* 1975;252:627–656. [PubMed: 1206570]
- Greenlee MW, Heitger F. The functional role of contrast adaptation. *Vision Research* 1988;28:791–797. [PubMed: 3227656]
- Heinrich TS, Bach M. Contrast adaptation in human retina and cortex. *Investigative Ophthalmology & Visual Science* 2001;42:2721–2727. [PubMed: 11581221]
- Hess RF, Bradley A. Contrast perception above threshold is only minimally impaired in human amblyopia. *Nature* 1980;287:463–464. [PubMed: 7432473]
- Hood, DC. Psychological and physiological tests of proposed physiological mechanism of light adaptation. In: Armington, JC.; Krauskopf, J.; Wooten, BR., editors. *Visual psychophysics and physiology*. New York: Academic; 1978. p. 141-155.
- Kohn A, Movshon JA. Neuronal adaptation to visual motion in area MT of the macaque. *Neuron* 2003;39:681–691. [PubMed: 12925281]
- Lagarias JC, Reeds JA, Wright MH, Wright PE. Convergence properties of the Nelder-mead simplex method in low dimensions. *SIAM Journal of Optimization* 1998;9:112–147.
- Laughlin SB. A simple coding procedure enhances a neuron's information capacity. *Z. Naturforschung* 1981;36:910–912.
- Laughlin, SB. Coding efficiency and visual processing. In: Blakemore, C., editor. *Vision: Coding and efficiency*. Cambridge: Cambridge University Press; 1990. p. 26-31.
- Legge GE. A power law for contrast discrimination. *Vision Research* 1981;21:457–467. [PubMed: 7269325]
- Legge GE, Foley JM. Contrast masking in human vision. *Journal of Optical Society of America* 1980;70:1458–1471.
- Li X, Lu ZL, Tjan BS, Doshier BA, Chu W. Blood oxygenation level-dependent contrast response functions identify mechanisms of covert attention in early visual areas. *Proceedings of the National Academy Sciences of the United States of America* 2008;105:6202–6207.
- Mei M, Leat SJ. Suprathreshold contrast matching in maculopathy. *Investigative Ophthalmology & Visual Science* 2007;48:3419–3424. [PubMed: 17591917]
- Murray SO. The effects of spatial attention in early human visual cortex are stimulus independent. *Journal of Vision* 2008;8(10):2, 1–11. <http://journalofvision.org/8/10/2/>
- Murray SO, He S. Contrast invariance in the human lateral occipital complex depends on attention. *Current Biology* 2006;16:606–611. [PubMed: 16546086]
- Nachmias J, Sansbury RV. Letter: Grating contrast: Discrimination may be better than detection. *Vision Research* 1974;14:1039–1042. [PubMed: 4432385]
- Naka KI, Rushton WA. S-potentials from luminosity units in the retina of fish (Cyprinidae). *The Journal of Physiology* 1966;185:587–599. [PubMed: 5918060]
- Ohzawa I, Sclar G, Freeman RD. Contrast gain control in the cat's visual system. *Journal of Neurophysiology* 1985;54:651–667. [PubMed: 4045542]
- Olman CA, Ugurbil K, Schrater P, Kersten D. BOLD fMRI and psychophysical measurements of contrast response to broadband images. *Vision Research* 2004;44:669–683. [PubMed: 14751552]
- Pelli, DG. The visual requirements of mobility. In: Woo, GC., editor. *Low vision: Principles and applications*. New York: Springer Verlag; 1987. p. 134-146.
- Pelli DG. The VideoToolbox software for visual psychophysics: Transforming numbers into movies. *Spatial Vision* 1997;10:437–442. [PubMed: 9176953]
- Pestilli F, Viera G, Carrasco M. How do attention and adaptation affect contrast sensitivity? *Journal of Vision* 2007;7(7):9, 1, 12. [PubMed: 17685805] <http://journalofvision.org/7/7/9/>
- Ross J, Speed HD. Contrast adaptation and contrast masking in human vision. *Proceedings of the Royal Society B: Biological Sciences* 1991;246:61–69.

- Rubin GS, Legge GE. Psychophysics of reading. VI—The role of contrast in low vision. *Vision Research* 1989;29:79–91. [PubMed: 2788957]
- Sclar G, Lennie P, DePriest DD. Contrast adaptation in striate cortex of macaque. *Vision Research* 1989;29:747–755. [PubMed: 2623819]
- Sereno MI, Dale AM, Reppas JB, Kwong KK, Belliveau JW, Brady TJ, et al. Borders of multiple visual areas in humans revealed by functional magnetic resonance imaging. *Science* 1995;268:889–893. [PubMed: 7754376]
- Simmers AJ, Bex PJ, Hess RF. Perceived blur in amblyopia. *Investigative Ophthalmology & Visual Science* 2003;44:1395–1400. [PubMed: 12601073]
- Smith AM, Lewis BK, Ruttimann UE, Ye FQ, Sinnwell TM, Yang Y, et al. Investigation of low frequency drift in fMRI signal. *Neuroimage* 1999;9:526–533. [PubMed: 10329292]
- Webster MA, Georgeson MA, Webster SM. Neural adjustments to image blur. *Nature Neuroscience* 2002;5:839–840.
- Wetherill GB, Levitt H. Sequential estimation of points on a psychometric function. *British Journal of Mathematical and Statistical Psychology* 1965;18:1–10. [PubMed: 14324842]
- Zenger-Landolt B, Heeger DJ. Response suppression in V1 agrees with psychophysics of surround masking. *Journal of Neuroscience* 2003;23:6884–6893. [PubMed: 12890783]

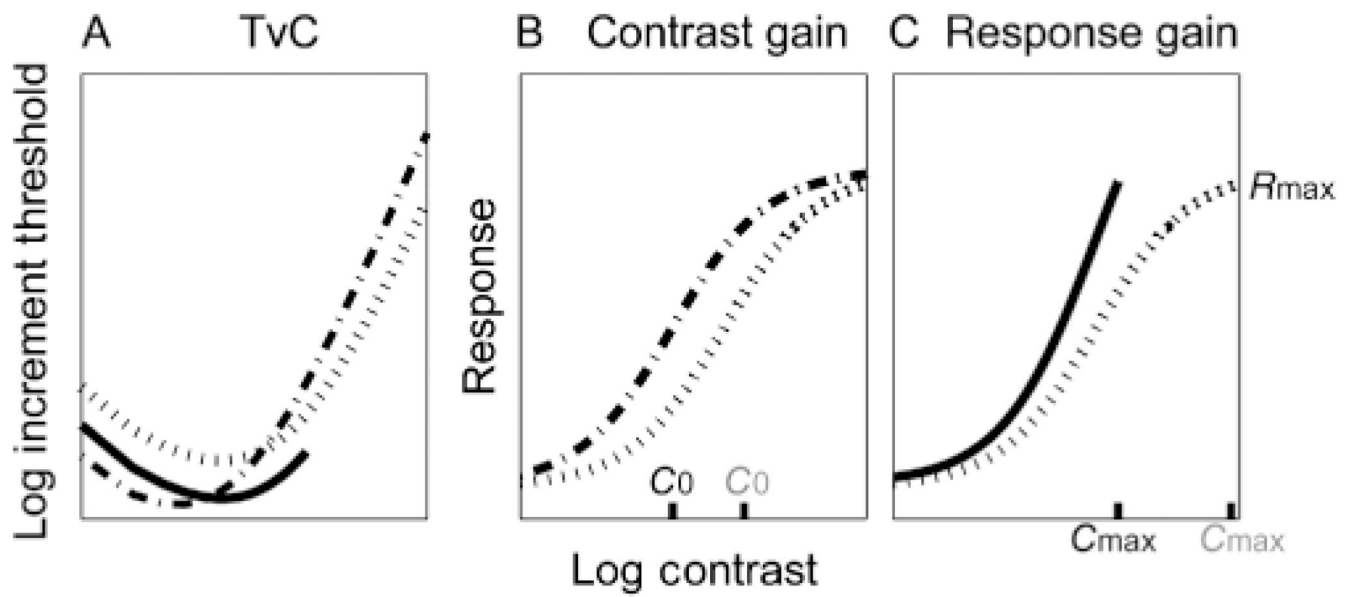


**Figure 1.**

Two potential mechanisms describing effects of prolonged contrast adaptation on Threshold vs. Contrast (TvC) functions and Contrast Response Functions (CRF): (A) TvCs; (B) CRF Contrast gain; (C) Response gain. Dotted lines indicate before adaptation, dashed line for contrast-gain and solid line for response-gain.

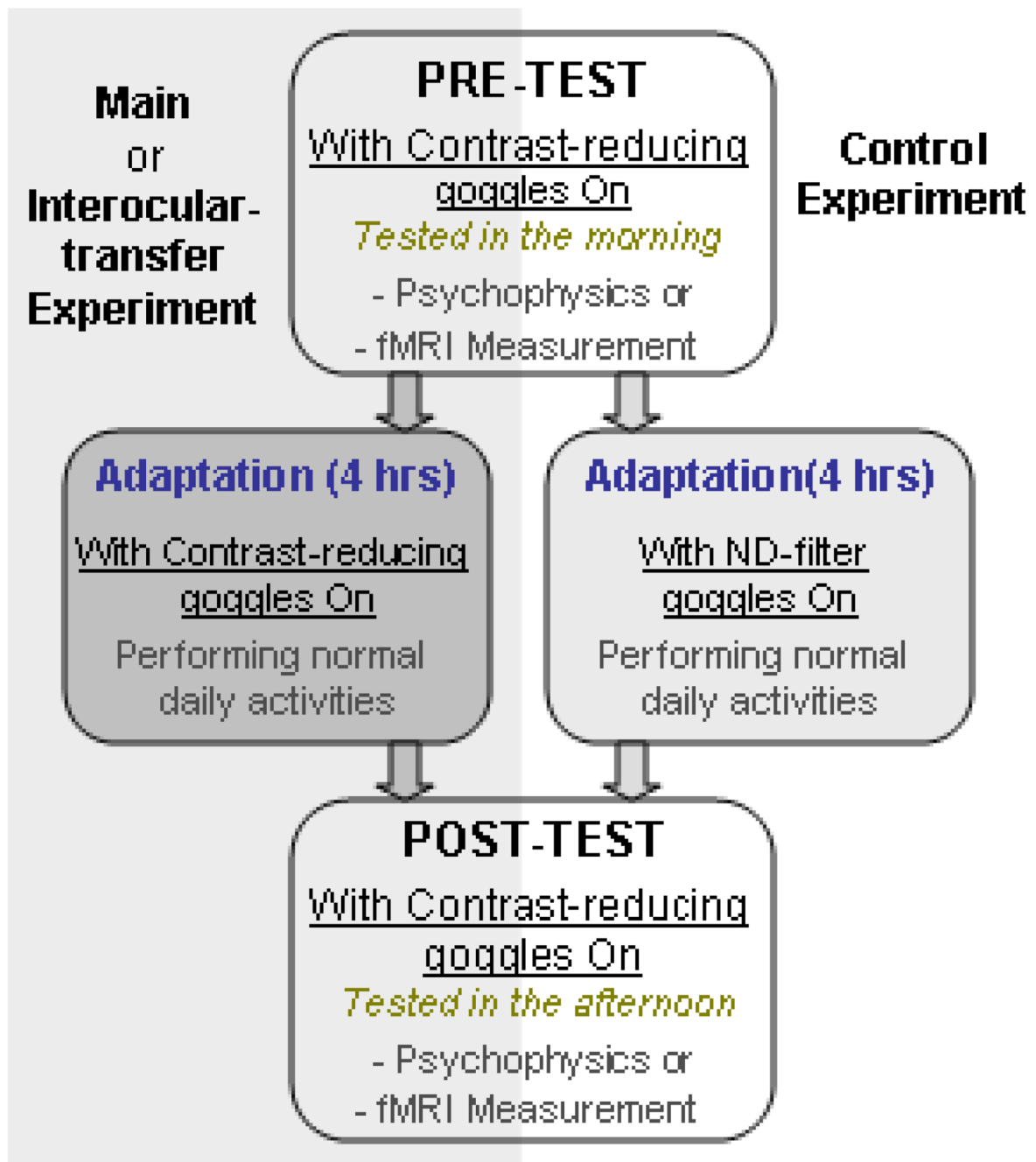


**Figure 2.**  
 Schematic diagram of experimental design.



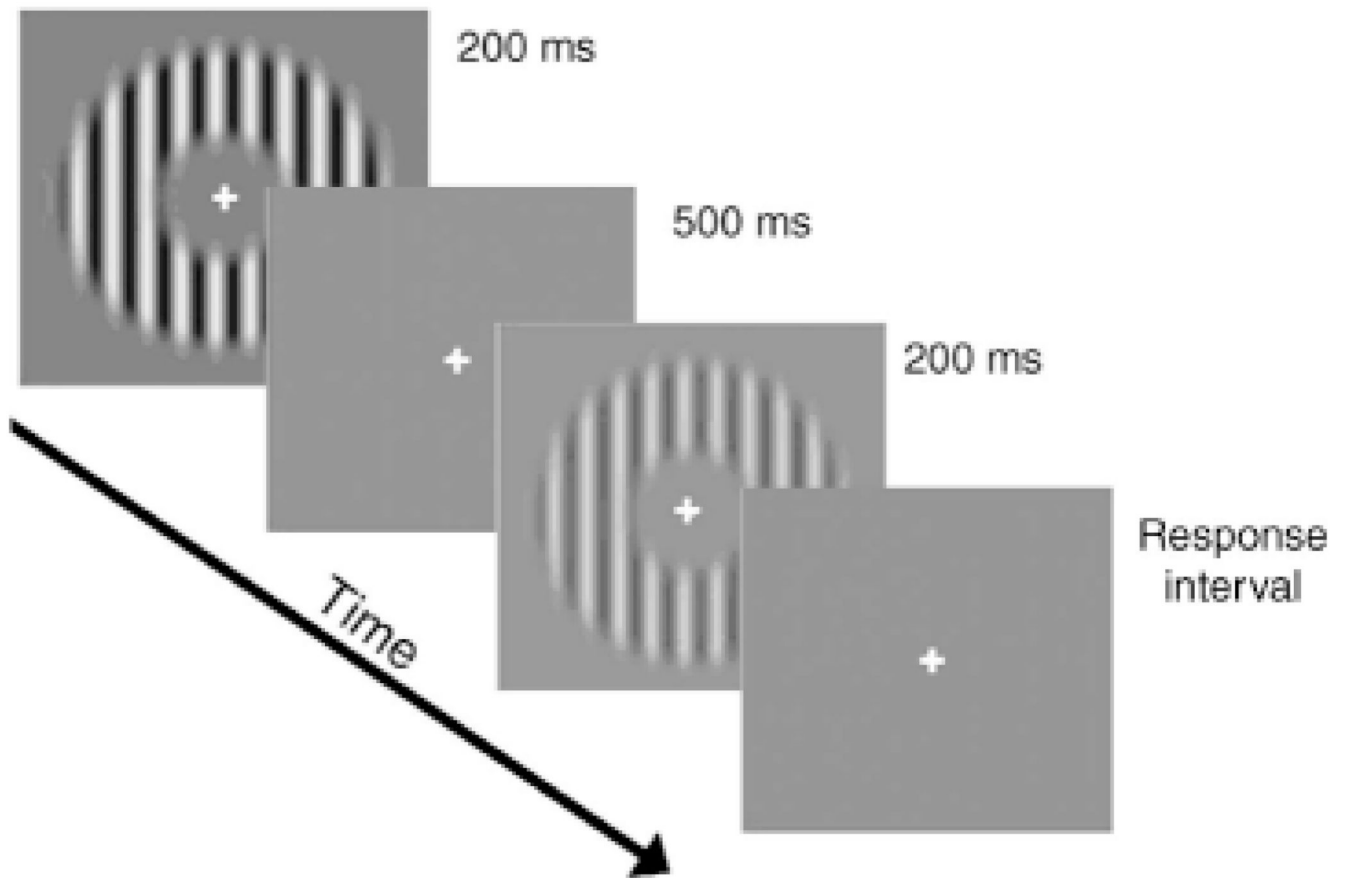


**Figure 3.**  
A schematic diagram of one trial in the contrast-discrimination task.

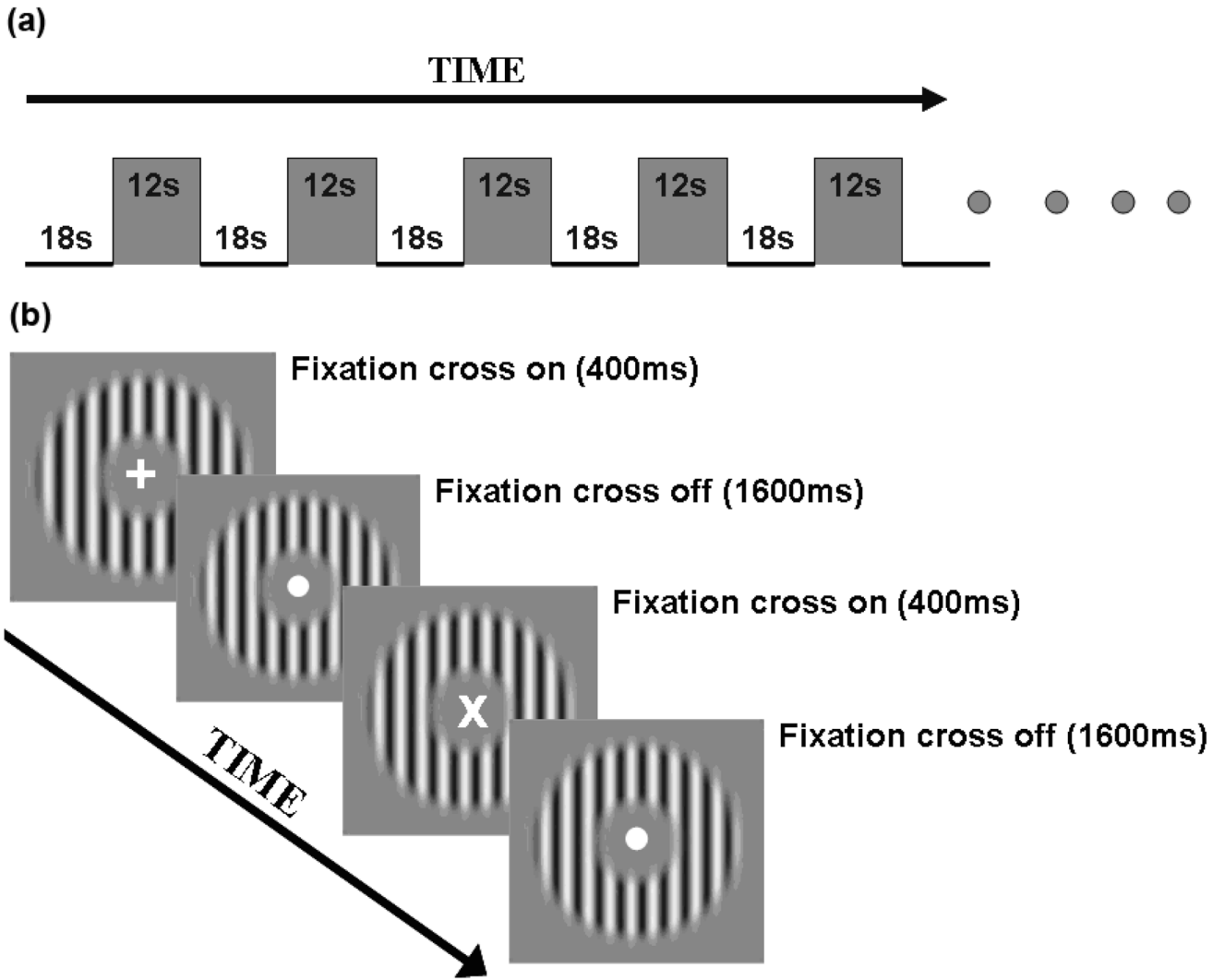


**Figure 4.** A schematic diagram of the block design for the fMRI contrast response task. The top panel (a) depicts the block design for one scan. The bottom panel (b) depicts the sequence of two test trials.

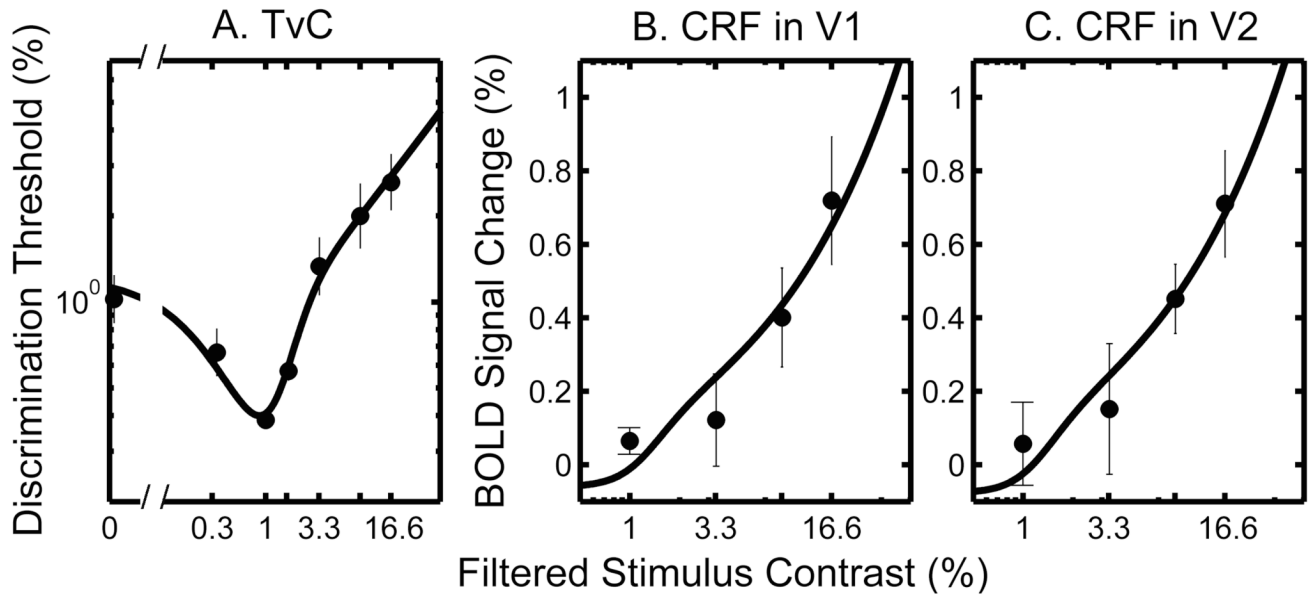


**Figure 5.**

Simultaneous fits to group averaged TvCs and fMRI CRFs in V1 and V2 respectively. Both TvC and CRF data are from the pre-test condition of the main experiment. (A) TvC. Discrimination thresholds (%) are plotted as a function of filtered pedestal contrast in log-log coordinates. Each data point represents the geometric mean of threshold estimates across subjects ( $n = 3$ ); (B) fMRI CRF in V1; (C) fMRI CRF in V2, averaged across subjects ( $n = 3$ ). The fMRI BOLD signal changes (%) are plotted as a function of filtered stimulus contrast in linear-log coordinates. The error bars represent 1 *SEM*. *Note:* The filtered contrast denotes the stimulus contrast taking into account attenuation by the contrast-reducing goggles. It is obtained by dividing the stimulus contrast on screen by a factor of 3.

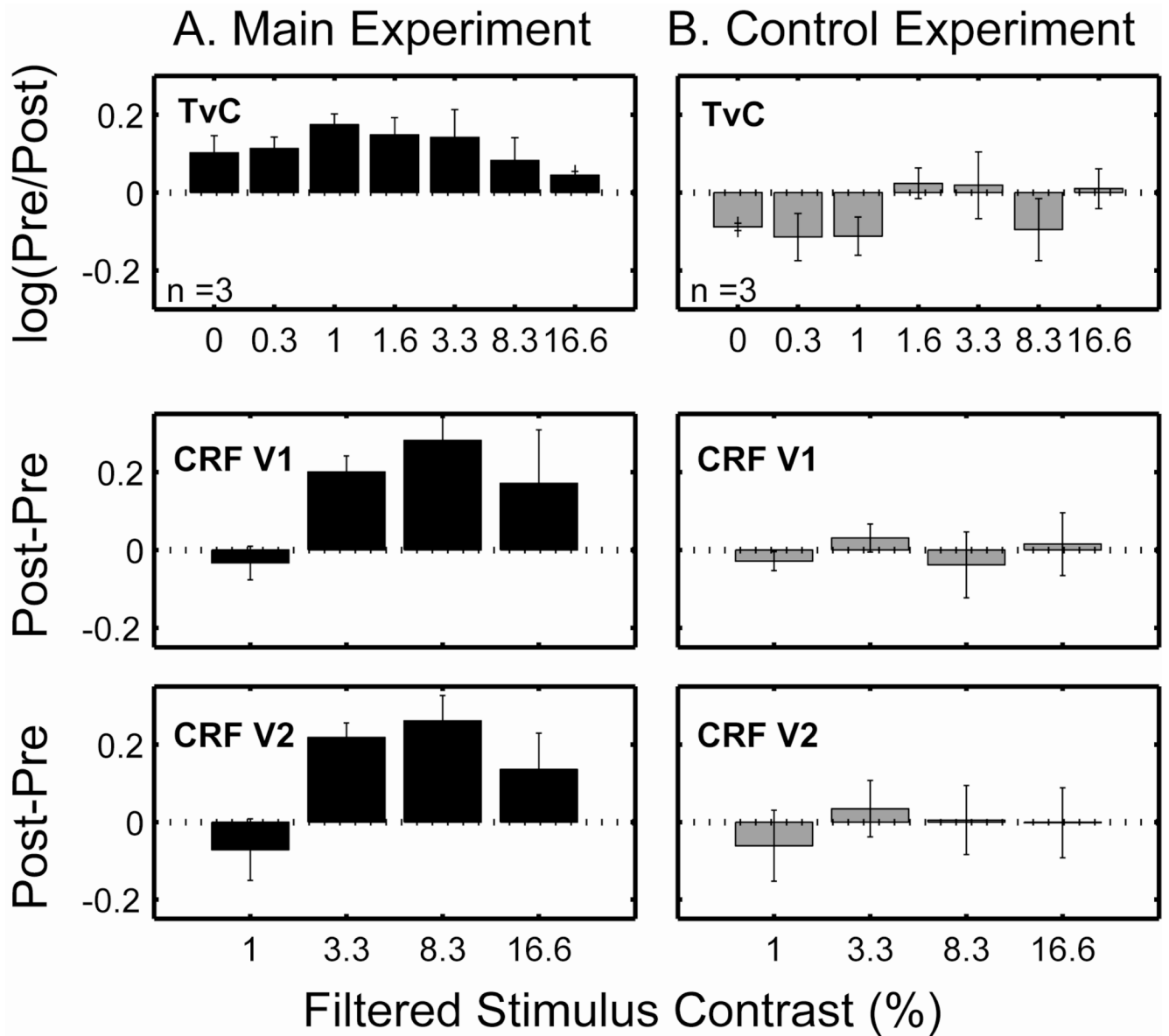


**Figure 6.**

Difference values (bar height) between pre- and post-tests as a function of stimulus contrast (first column for the main experiment and second column for the control experiment): TvCs (first row), CRFs in V1 (second row), and CRFs in V2 (third row). The horizontal dashed lines represent no pre-post difference (value of 0). The error bars represent 1 SEM.

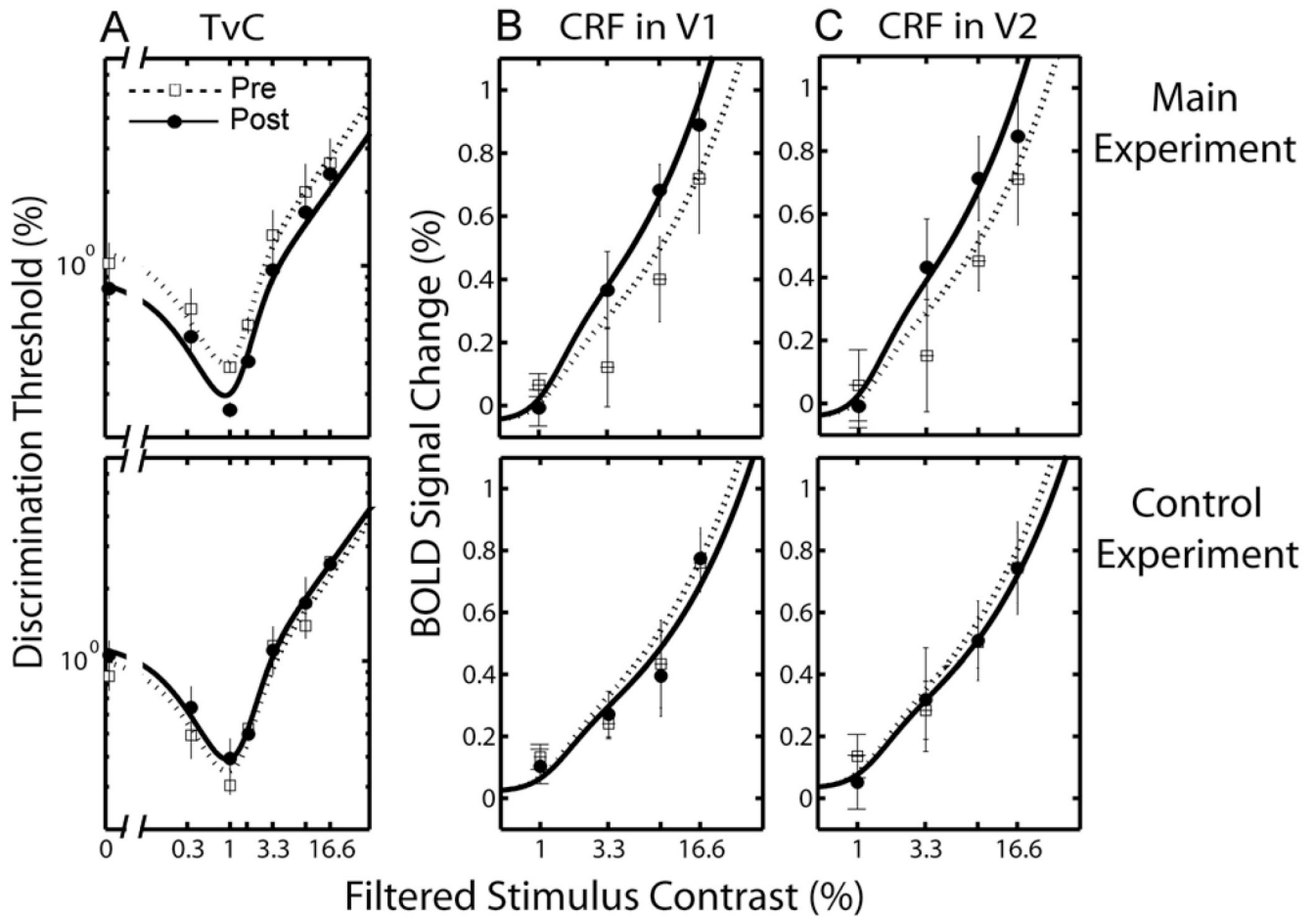


**Figure 7.**

TvCs and fMRI BOLD CRFs (*Top panels*: main experiment, *Bottom panels*: control experiment): (A) TvC functions, averaged across subjects ( $n = 3$ ). Discrimination thresholds (%) are plotted as a function of filtered pedestal contrast in log-log coordinates. Each panel contains two TvC functions, one from the pre-test (open squares), and one from the post-test (closed circles); (B) fMRI BOLD CRFs in V1 and (C) V2, averaged across subjects ( $n = 3$ ). The fMRI BOLD signal changes (%) are plotted as a function of filtered stimulus contrast in linear-log coordinates. The open squares represent the CRF from the pre-test and the closed circles for the CRF from the post-test. The error bars represent 1 *SEM*. Smooth curves are the predictions of the best fitting model (i.e., response gain).

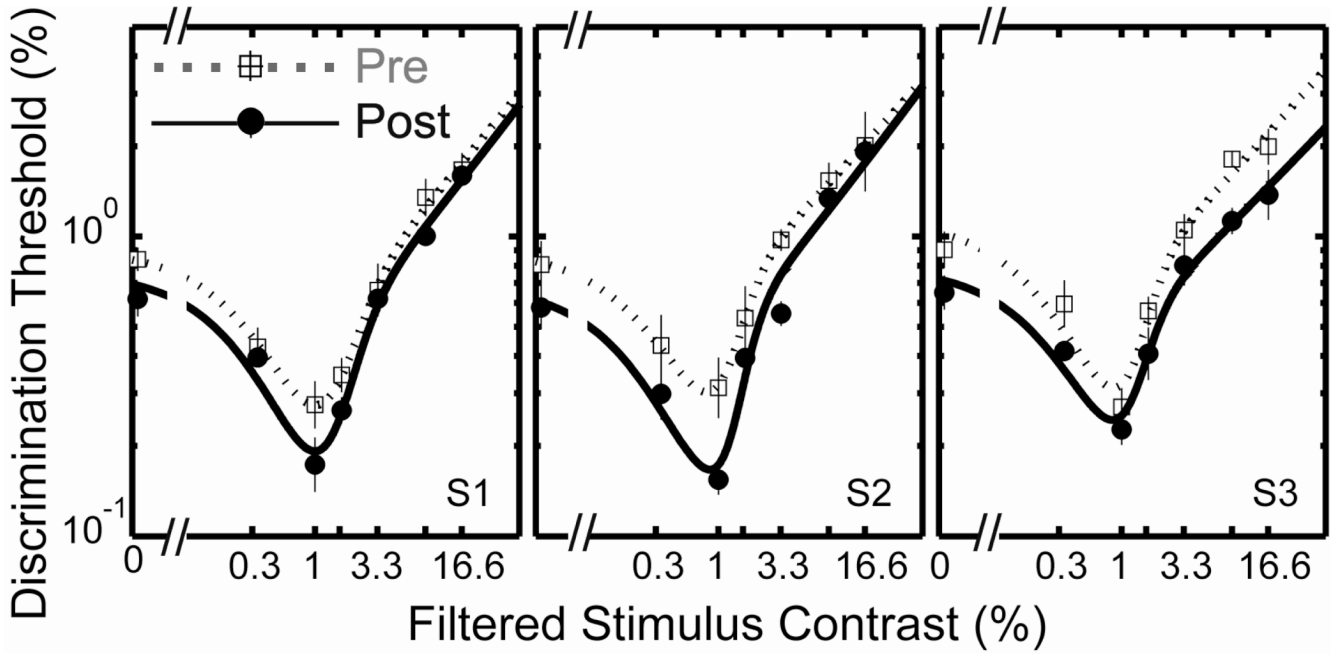


**Figure 8.** Contrast discrimination functions showing that the adaptation effect exhibits interocular transfer. Each panel shows data from one subject and contains two TvC functions measured in the eye that is occluded by a translucent occluder during the four-hour adaptation period: one from the pre-test (dotted line with open squares) and the other from the post-test (solid line with closed circles). Each data point represents the geometric mean of four threshold estimates, each derived from a forced-choice staircase. Each error bar represents 1 SEM.



**Table 1**

Log contrast sensitivity and visual acuity for the tested eye of each participant with/without the contrast-reducing goggles.

		S1	S2	S3
<b>Log Contrast Sensitivity</b>	Without goggles	1.90	2.05	1.65
	With goggles	1.30	1.60	1.15
<b>Visual Acuity (logMAR)</b>	Without goggles	0.14	0.02	0.24
	With goggles	0.20	0.06	0.32

Mean parameter values ( $n = 3$ ) fit simultaneously to the TvC and CRF data (based on data from the pre-test condition of the main experiment).

**Table 2**

Cortical Area	$R_{max}$	$n$	$m$	$C_{50}$	$\Delta R_c$	TvC $RSS_{error}$	CRF $RSS_{error}$	Total $RSS_{error}$
V1	2.63 ( $\pm 0.14$ )	3.60 ( $\pm 0.23$ )	0.54 ( $\pm 0.05$ )	1.24 ( $\pm 0.08$ )	0.06 ( $\pm 0.01$ )	0.09 ( $\pm 0.03$ )	0.04 ( $\pm 0.03$ )	0.13 ( $\pm 0.05$ )
V2	2.68 ( $\pm 0.19$ )	3.59 ( $\pm 0.24$ )	0.53 ( $\pm 0.04$ )	1.25 ( $\pm 0.07$ )	0.06 ( $\pm 0.01$ )	0.09 ( $\pm 0.03$ )	0.07 ( $\pm 0.05$ )	0.16 ( $\pm 0.07$ )

**Table 3**

Parameters of the best fitting model in V1 and V2 areas.

Cortical Area	Test	$R_{max}$	$n$	$m$	$C_{50}$
V1	Pre-test	2.8223 ( $\pm 0.0011$ )	3.5588	0.5091	1.2887
	Post-test	3.6893 ( $\pm 0.0018$ )	( $\pm 0.0017$ )	( $\pm 0.0004$ )	( $\pm 0.0007$ )
V2	Pre-test	2.8252 ( $\pm 0.0011$ )	3.5585	0.5088	1.2892
	Post-test	3.6875 ( $\pm 0.0019$ )	( $\pm 0.0017$ )	( $\pm 0.0004$ )	( $\pm 0.0007$ )